frontiers | Frontiers in Materials

ORIGINAL RESEARCH
published: 12 July 2022
doi: 10.3389/fmats.2022.927806

Scaled Fracture Toughness Based on the Weibull Stress for the Ferritic Steel Used in Nuclear Power Plants

Weiya Jin[1,2], *Yan Li*[2], *Yuebing Li*[1,2] *and Mingjue Zhou*[1,2]*

[1]*Institute of Process Equipment and Control Engineering, Zhejiang University of Technology, Hangzhou, China,* [2]*College of Mechanical Engineering, Zhejiang University of Technology, Hangzhou, China*

As an important material property in structural integrity assessment of nuclear power components, fracture toughness can be measured by single edge-notched bend (SENB) specimens or compact tension (CT) specimens. However, the tested values may be inhomogeneous with the crack size and specimen thickness. Some toughness scaling models (TSMs) were proposed to transfer the tested value to fracture toughness under small-scale yielding. Combined with the tested data by SENB specimens with different crack sizes and CT specimens with different thicknesses, the scaled fracture toughness is investigated on the global and local approaches to fracture. Using the scaled toughness values, the Weibull scale parameter K_0 is estimated and compared for the ferritic steel DIN 22NiMoCr37 widely used in nuclear power plants. The results show that the estimated scale parameter K_0 using the scaled toughness obtained by the global approach on the *J-Q* theory is reasonable in agreement with that of the local approach on the Weibull stress with a relative error of about 10%.

Keywords: toughness scaling models, ferritic steel, local approach to fracture, Weibull stress, *J-Q* theory

OPEN ACCESS

Edited by:
Zihao Wang,
Tohoku University, Japan

Reviewed by:
Kehuan Wang,
Harbin Institute of Technology, China
Jianhua Pan,
Hefei University of Technology, China

***Correspondence:**
Mingjue Zhou
zhoumingjue@zjut.edu.cn

Specialty section:
This article was submitted to Environmental Degradation of Materials, a section of the journal Frontiers in Materials

Received: *25 April 2022*
Accepted: *31 May 2022*
Published: *12 July 2022*

Citation:
Jin W, Li Y, Li Y and Zhou M (2022) Scaled Fracture Toughness Based on the Weibull Stress for the Ferritic Steel Used in Nuclear Power Plants. Front. Mater. 9:927806. doi: 10.3389/fmats.2022.927806

1 INTRODUCTION

Fracture toughness is a very important characteristic of a structural material indicating the resistance of a material to cracks, which is an indispensable input in the structural intensity assessment of nuclear power components containing cracks. As a key component in nuclear power plants, reactor pressure vessels are usually manufactured using ferritic steels, which presents a significantly ductile–brittle transition. In addition, the embrittlement effect caused by irradiation will increase the ductile–brittle transition temperature, which brings about the failure risk of brittle fracture.

Several geometry configurations can be used to measure the value of fracture toughness, including the single edge-notched bend (SENB) specimens or compact tension (CT) specimens, which are recommended in the test standards such as ASTM E1820 (ASTM International, 2020) and ISO 12135 (International Organization for Standardization, 2016). However, the fracture resistance depends on the specimen thickness and crack length, usually characterized by the out-of-plane and in-plane constraints on the macroscopic fracture mechanics. Some special provisions in the specimen thickness and crack length have been restricted in these test standards to obtain an effective value of fracture toughness for engineering assessment. It should be noted that the tested fracture toughness may be varied with the specimen configuration. Therefore, some toughness scaling models (TSMs) have been proposed to transfer the tested value to fracture toughness under small-scale yielding.

In order to explain the effect of crack length on the fracture toughness, a TSM is first proposed to transfer the tested value with a certain crack length to that with another crack size, with an assumption of the same critical stress on the crack head under plane strain (Dodds et al., 1991). Lately, O'Down and Shih proposed the *J-Q* theory to describe the stress field near the crack tip (O'dowd and Shih 1992; O'Dowd, 1995). The *Q*-parameter is now usually used to characterize the in-plane constraint due to the crack length. Compared with the crack opening stress, the fracture load for a certain specimen can be determined with the in-plane constraint parameter *Q*. Then, the fracture toughness can be scaled from different constraints. A model with *T*-stress to account for the in-plane constraint is provided in the R6 procedure (EDF Energy Nuclear Generation Ltd, 2015) for engineering practice. In addition, Ishihara et al. (2017) and Meshii and Ishihara (2018) proposed a T-scaling method for stress distribution scaling under small-scale yielding to scale the fracture toughness with the consideration of temperature dependence.

However, the toughness scaling models based on 2D plane strain models under small-scale yielding tend to overpredict the increment in toughness due to a loss of constraint (Link and Joyce, 1996). The thickness effect on the fracture toughness should be considered, which is usually described with the fracture toughness J_c corrected proportionally to the −1/2 power of thickness (Anderson et al., 1994). With the development of 3D crack-front stress fields, Guo (1995) and She and Guo (2007) introduced a parameter T_z as a function of thickness, which is successfully used to describe the effect of out-of-plane constraint on the fracture toughness. It should be noted that either parameter *Q* or T_z is usually limited to quantifying the in-plane or out-of-plane constraint separately. Several unified measure parameters of constraint are proposed to describe both in-plane and out-of-plane constraints, such as A_c (Mostafavi et al., 2010; Mostafavi et al., 2011; Nikishkov and Matvienko, 2016), A_p (Yang et al., 2013; Ma et al., 2016), and A_d (Xu et al., 2018; Zhen et al., 2021). It has been verified that these parameters can effectively characterize both in-plane and out-of-plane constraints.

In the above global approaches, the mean values of fracture toughness are usually focused, which has difficulty in explaining the scatter of the cleavage fracture toughness over the ductile–brittle transition (DBT) region. The local approach to fracture based on Weibull stress (Ruggieri and Dodds, 2018) can be used to describe the statistics feature of fracture toughness by a Weibull distribution. Then, one can scale the fracture toughness for constraint correction between cracked specimens of differing constraint levels with the same Weibull stress. In addition, the cleavage fracture probability can be calculated using the Weibull stress under different loading levels. Using local criterion based on the equivalence of Weibull stress, Ruggieri and Dodds (1996) successfully predicted the combined effects of loss of constraint. Gao et al. (1998), Gao and Dodds (2000), and Gao and Dodds Jr (2001) gave a simplified approach to assess constraint effects on cleavage fracture toughness of ferritic steels in the DBT region under plane strain, small-scale yielding conditions. A non-dimensional *T*-function is built up to scale fracture toughness values for constraint loss on the Weibull stress model. Based on Weibull stress, Smith et al. (2018) proposed an energy scaling mode to accurately predict cleavage fracture at quasi-static loading rates. The effect of blunt notches with varying root radii on the fracture behavior of SE(B) specimens is investigated using the Weibull stress-based toughness scaling model by Horn and Sherry (2010). The results show that different Weibull parameters will be obtained using notched specimens and conventional specimens containing pre-cracks. The test data and FE modeling results indicate that the effect of out-of-plane constraint loss on notch fracture toughness can be of the same order of magnitude as the in-plane effect of the notch radius alone (Horn et al., 2020). The local approach based on Weibull stress is also used to scale the fracture toughness of the sub-size specimens and compared with the standard specimens (Qian et al., 2018a; Ruggieri, 2020; Pan and Yin, 2021). Recently, Barbosa and Ruggieri (2020) investigated the thickness effect on fracture toughness based on the TSMs using the Weibull stress.

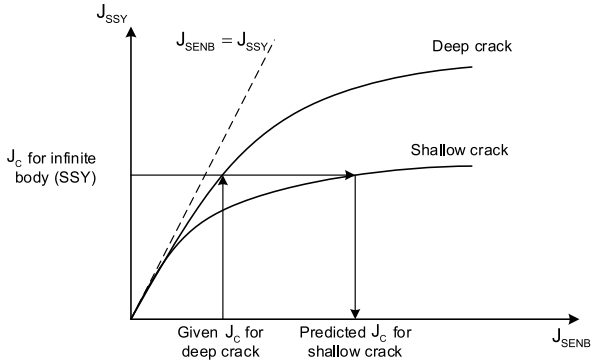

FIGURE 1 | Schematic of the relationship between the J-integral values in SENB specimens for deep and shallow cracks with those of SSY conditions which generate equivalent opening mode stresses ahead of the crack tip.

The fracture toughness from different constraint levels can be scaled by these TSMs developed by the global approach on the critical stress or the local approach on the Weibull stress. Therefore, the differences among these TSMs are compared and discussed in this work. **Section 2** gives some detailed descriptions of the two types of TSMs. The data of fracture tests and finite element models are shown in **Section 3**. The scaled values of fracture toughness are obtained and discussed in **Section 4**. The last section gives some conclusions.

2 TOUGHNESS SCALING MODELS

2.1 Global Approach to *J-Q* Theory

The variations in fracture toughness resulting from the loss of constraint due to crack length are usually scaled by a 2D small-scale yielding (SSY) model. According to the critical stress, the scaling model compares the stress distribution in the tested

specimen geometry with that of an infinite body under SSY, especially for the crack opening stress (Dodds et al., 1991). Then, the tested fracture toughness J_{IC} by specimens can be transferred to the effective fracture toughness J_{SSY} with the 2D SSY model, which denotes equivalent driving force for cleavage fracture on the critical stress over a microstructurally relevant volume. The effect of crack length on the fracture toughness tested by SENB specimens was successfully accounted for by the 2D SSY model. The tested fracture toughness results of deep crack specimens with a high constraint can be appropriately scaled for that of shallow crack specimens or structures with low constraint, as shown in **Figure 1**.

The two-parameter *J-Q* theory can describe the near tip stress and strain states in a range of crack tip geometries. Parameter *Q* is determined from a finite element analysis and is the difference between the actual hoop stress and reference field hoop stress as follows:

$$Q = \frac{(\sigma_{22})_{\mathrm{FEM}} - (\sigma_{22})_{\mathrm{MBL}}}{\sigma_0} \quad \text{at } r = 2J/\sigma_0\,, \tag{1}$$

where $(\sigma_{22})_{FEM}$ is the stress distribution computed by the finite element method and $(\sigma_{22})_{MBL}$ is the stress distribution computed according to the boundary layer approach with the assumption of SSY. Parameter *Q* based on crack-tip stress fields is widely used to characterize the levels of in-plane constraint in specimens or structures. According to the measured value J_C, a scaled fracture toughness J_{CQ} with the constraint *Q* can be predicted as (O'dowd and Shih, 1992)

$$\frac{J_{\mathrm{CQ}}}{J_{\mathrm{C}}} = \left(1 - \frac{Q}{\sigma_{\mathrm{c}}/\sigma_0}\right)^{n+1}. \tag{2}$$

The critical stress σ_c can be calculated according to the test results with different in-plane constraints. σ_0 is the yield stress and n is the hardening exponent in the Ramberg–Osgood constitutive relation.

With the assumption of finite strains, Neimitz et al. (2007) gave a modified scaling model on O'Dowd's formula and generalized it for the arbitrary reference state. The corrected fracture toughness J_{CQ} by the *Q* parameter can be calculated by

$$\frac{J_{\mathrm{CQ}}}{J_{\mathrm{C}}} = \left(\frac{\sigma_{22}^{\max} - Q\sigma_0}{(\sigma_{22}^{\max})_{\mathrm{ref}} - Q_{\mathrm{ref}}\sigma_0}\right)^{n+1}, \tag{3}$$

where J_C is the fracture toughness measured by a specimen with the reference state Q_{ref}. σ_{22}^{max} is the maximum opening stress in front of the crack, computed numerically under the assumption of finite strains.

For the thickness effect, Guo et al. proposed the T_z parameter to describe the 3D stress distribution in front of the crack, which can be used to consider the influence of the out-of-plane constraint on the fracture toughness. Consistent with the *Q* parameter for in-plane constraint, the corrected fracture toughness J_{CQ} by the T_z parameter can be calculated by (Neimitz and Dzioba, 2015)

$$\frac{J_{\mathrm{CQ}}}{J_{\mathrm{C}}} = \left(\frac{I_n(T_z, n)}{I_n\big((T_z)_{\mathrm{ref}}, n\big)}\right)\left(\frac{\tilde{\sigma}_{22}\big((T_z)_{\mathrm{ref}}, n, \theta = 0\big)}{\tilde{\sigma}_{22}(T_z, n, \theta = 0)}\right)^{n+1}, \tag{4}$$

where $\tilde{\sigma}_{22}$ and I_n are constants for the HRR stress distribution and ν is Poisson's ration.

For the effect of thickness under the same in-plane constraint Q, the fracture toughness can be corrected using parameter T_z as (Guo, 1995; Neimitz and Galkiewicz, 2006; Zhao and Guo, 2012)

$$\frac{J_{\mathrm{CQ}}}{J_{\mathrm{C}}} = \frac{\frac{2}{3}(1+\nu) + \frac{4}{3}(1-2\nu)\left(\frac{1+T_z(B_{\mathrm{ref}})}{1-2T_z(B_{\mathrm{ref}})}\right)^2}{\frac{2}{3}(1+\nu) + \frac{4}{3}(1-2\nu)\left(\frac{1+T_z(B)}{1-2T_z(B)}\right)^2}. \tag{5}$$

Neimitz and Lipiec (2021) assumed that the Q parameters along the crack front depend on the T_z parameter and proposed a corrected fracture toughness procedure, considering both the out-of-plane and in-plane constraints. The key to the procedure is to compute the *Q* parameter in the specialized layer where the weighted average value of the T_z parameter is located. Then, we can use the 2D SSY model to scale the fracture toughness with the *Q* parameter as a function of the T_z parameter.

2.2 Local Approach to Weibull Stress

The fracture toughness presents a significant scatter over the DBT region. In order to quantify the statistic characterization, the local approaches employ a probabilistic model to define the functional relationship between macro- and microscale driving forces for cleavage fracture by using the scalar Weibull stress σ_W. The Weibull stress is calculated by integrating a weighted value of the maximum principal stress over the fracture process zone, as first proposed by Beremin. In the local approach, a two-parameter Weibull distribution is applied to describe the scatter of fracture toughness. The failure probability P_f is described as

$$P_{\mathrm{f}} = 1 - \exp\left(-\frac{\sigma_W}{\sigma_{\mathrm{u}}}\right)^m, \tag{6}$$

with the Weibull stress σ_W,

$$\sigma_{\mathrm{W}} = \left(\frac{1}{V_0}\int_{V_{\mathrm{FPZ}}} \sigma_1^m dV\right)^{1/m}, \tag{7}$$

where σ_u and m are the two model parameters known as Weibull modulus and the scale parameter, respectively. σ_1 is the maximum tensile principal stress, V_0 is a reference volume, and V_{FPZ} is the volume in the fracture process zone (FPZ). Therefore, the Weibull stress is a synthetical scaling parameter, including the effect of in-plane and out-of-plane constraints.

Figure 2 shows the construction of the toughness scaling model based on Weibull stress. In general, we can obtain the test value of fracture toughness using a specimen with configuration A, denoted as J_C^A. Then, the maximum principal stress distribution can be calculated based on finite element analysis using the specimen with configuration A under the loading J_C^A. According to the local approach, the critical Weibull stress $\sigma_{W,C}$ can be evaluated by **Eq. 7**, as shown in **Figure 2A**. Meanwhile, the loading can be determined using the specimen with configuration A for the critical Weibull stress $\sigma_{W,C}$, which is the scaled fracture

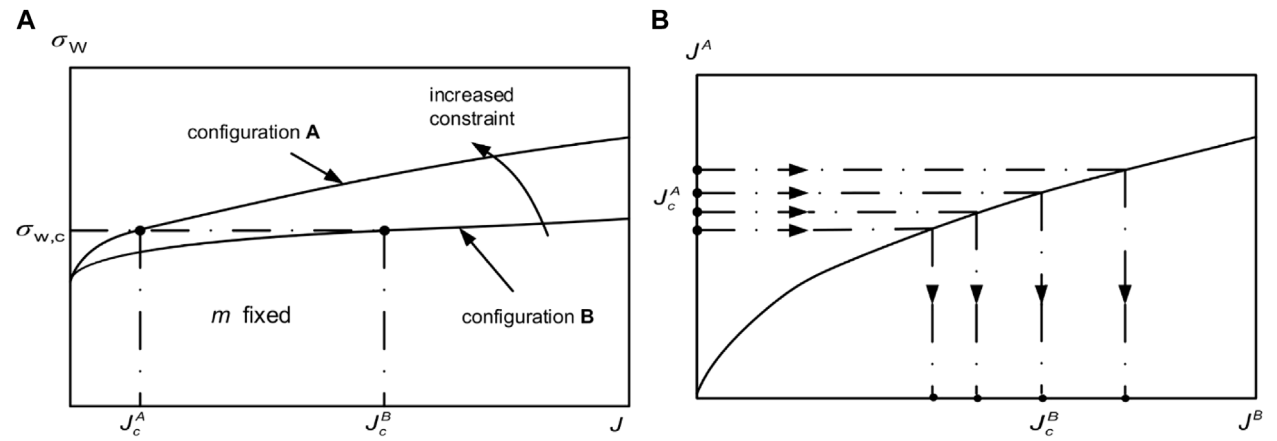

FIGURE 2 | Illustration of toughness scaling between specimen configurations A and B based on the Weibull stress. **(A)** Loading J-integrity vs. Weibull stress. **(B)** Scaled fracture toughness from J_c^A to J_c^B.

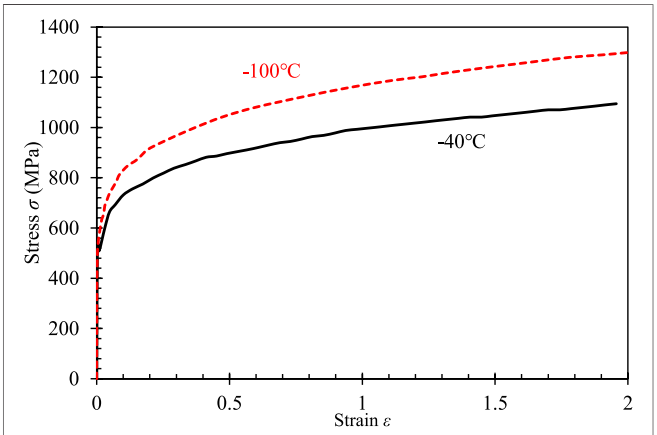

FIGURE 3 | True stress–strain curves at −100°C and −40°C.

toughness J_C^B. For the series of tested toughness values J_C^A, the scaled fracture toughness J_C^B can be determined, as shown in **Figure 2B**.

3 FRACTURE TESTS AND FINITE ELEMENT MODELS

3.1 Fracture Tests

In order to investigate the constraint effect on fracture toughness, several fracture toughness test results by CT and SENB specimens have been reported. For the ferritic steel DIN 22NiMoCr37 widely used in nuclear power plants, nearly 800 fracture toughness tests were performed using CT specimens to study specimen size and temperature effects on cleavage fracture toughness in the ductile–brittle fracture transition regime (Heerens and Hellmann, 2002). Using the same material, Gao et al. (2008) conducted fracture toughness tests by SENB specimens with $a/W = 0.1$ and 0.5 at −100°C. Thereby the tested results from these CT specimens and SENB specimens are used in this work to scale the fracture toughness. **Figure 3** shows the true stress-strain curves transferred from the tension tests of DIN 22NiMoCr37, as reported by Gao et al. (2008) and Wasiluk et al. (2006), which will be used in finite element analysis.

3.2 Finite Element Models

In this work, three kinds of specimen configurations are modeled by the finite element method using ABAQUS 2018, including the plane MBL, SENB, and CT models, as shown in **Figure 4**. For the MBL model used to model the SSY under plane strain, a detailed description can be found in previous studies (Li et al., 2019; Zhou et al., 2021). For the SENB and CT specimens, the quarter-symmetric models are considered with the sizes listed in **Table 1**, in which B is the specimen thickness, W denotes the specimen width, and a is the crack length.

Consistent with the crack tip in the MBL model, the crack tip with a radius $\rho_0 = 3$ mm is adopted to calculate the Weibull stress using plane strain element CPE8R with 6017 nodes and 1916 elements. The three-dimensional, eight-node linear element C3D8 is used to mesh the SENB and CT models with about 30,100 nodes and 25,100 elements. In order to investigate the effect of thickness, 15 layers are arranged over the half-thickness.

On the symmetry planes at $z = 0$, a symmetry condition is applied. In addition, the roller is fixed in the SENB specimen. These finite element models are loaded by displacement increments imposed on the loading points for the symmetry plane. Using the domain integral procedure, ABAQUS can calculate and output the local J values at the tip location along the crack front.

4 RESULTS AND DISCUSSIONS

4.1 Test Results

The tested values of fracture toughness J are first described in terms of K_J using a plane strain conversion:

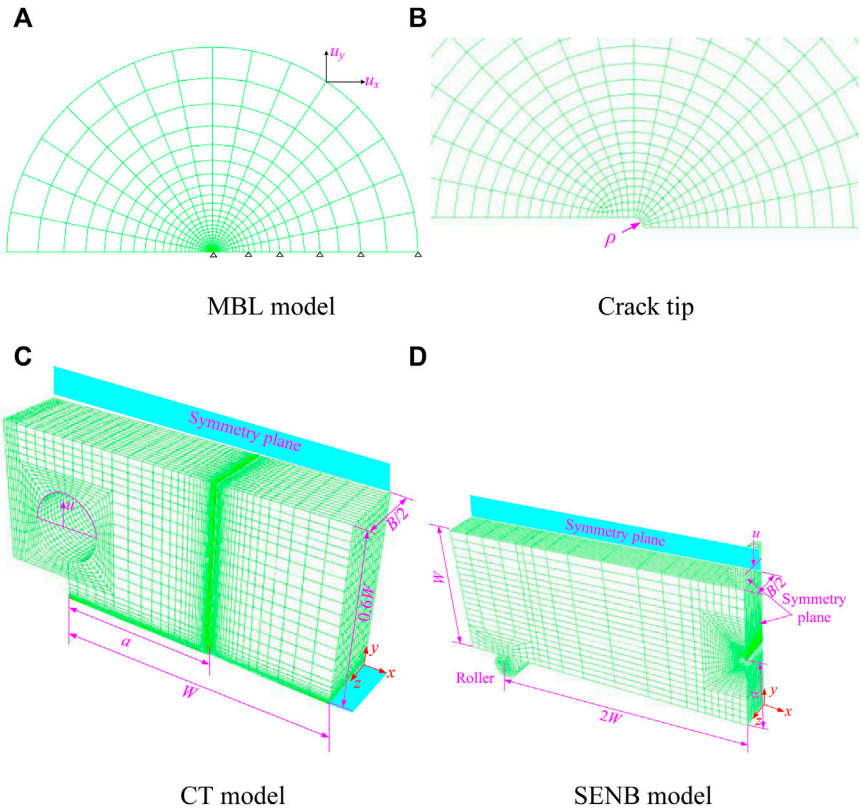

FIGURE 4 | Finite element models. **(A)** MBL model. **(B)** Crack tip. **(C)** CT model. **(D)** SENB model.

TABLE 1 | Geometry sizes used in FE models.

Specimen	*B* (mm)	*W*/*B*	*a*/*W*
SENB	25	2	0.1, 0.5
CT	12.5, 25, 50	2	0.57

$$K_{JC} = \sqrt{\frac{EJ}{1-\nu^2}}. \tag{8}$$

Then, the tested values of fracture toughness K_J with the rank probabilities are plotted in **Figure 5**. The rank probabilities are calculated by

$$P_f(i) = \frac{i - 0.3}{n + 0.4}, \tag{9}$$

where n denotes the number of toughness values in each data set and i represents the rank number. It can be obviously found that the crack length of single edge-notched bend (SENB) specimens and the thickness of CT specimens have an important effect on the fracture toughness. Higher fracture toughness presents in the lower in-plane constraint with shallow crack ($a/W = 0.1$) for SENB specimens or the lower out-of-plane constraint with thick CT specimens. Meanwhile, the scatter of test data by the same specimen geometry can be found with a maximum deviation of about 230Mpa$\sqrt{m}$ by the CT specimens with the thickness of 0.25T at −40°C. It is necessary to determine a scaled fracture toughness for the structural integrity assessment.

4.2 Toughness Scaled by Constraint Parameters *Q* and T_z

For the in-plane constraint, parameter Q is first calculated by the comparisons with the stress field of SENB specimens and MBL models, according to **Eq. 1**. **Figure 6** shows the in-plane constraint parameter Q with load levels at locations over the crack front. Nevalainen and Dodds (1996) stated that Q-values for the SENB specimen show an immediate loss of constraint with increased loading, especially at the surface point with $z = B/2$. Compared with the specimen with a shallow crack $a/W = 0.1$, Q-values for the specimen with a deep crack $a/W = 0.5$ exist higher constraint level at the center of the specimen thickness. Therefore, the specimen configuration with a deep crack $a/W = 0.5$ is recommended in most test standards.

Figure 7 shows the relationship of the local J values at the crack front and the scaled J values under SSY condition J_{SSY}. There is a significant difference in the scaled fracture toughness between the surface with $z = B/2$ and the midplane with $z = 0$ due to the constraint levels. The scaled fracture toughness will strongly depend on the selected thickness location. Generally, a Q-value at the midplane of the specimen or a specimen with the

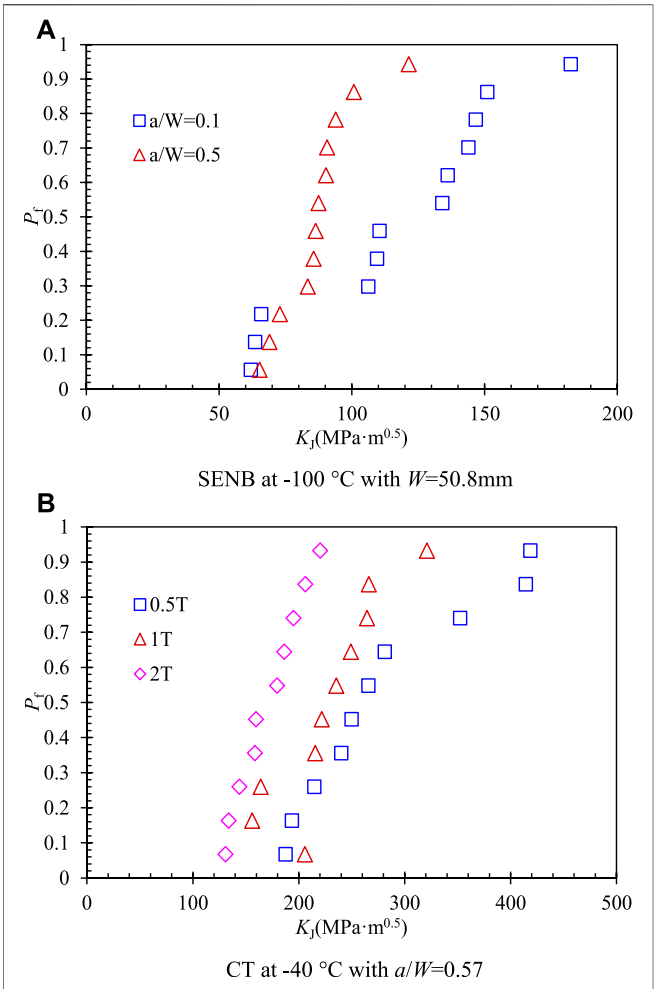

FIGURE 5 | Rank probabilities of fracture toughness data **(A)** SENB at −100°C with W = 50.8 mm. **(B)** CT at −40 °C with a/W = 0.57.

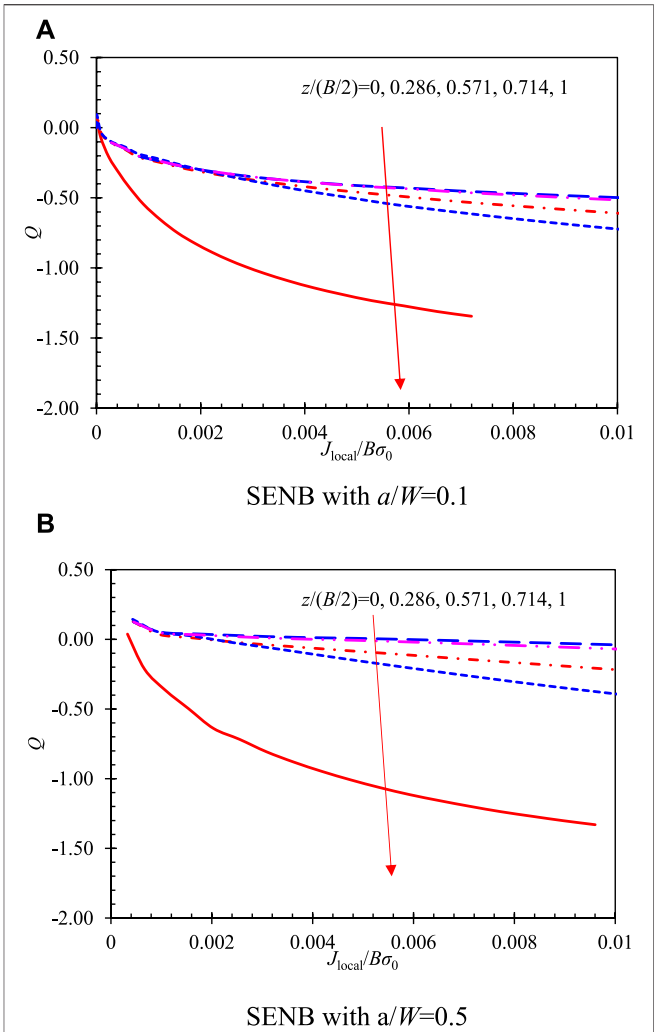

FIGURE 6 | Variation in Q with increased loading over the crack front. **(A)** SENB with a/W = 0.1. **(B)** SENB with a/W = 0.5

assumption of plane strain is adopted to scale the fracture toughness. Therefore, a large J_{SSY} will be predicted using the highest constraint level, whereas the other locations have low constraint levels. Therefore, it is necessary to determine the crack front location, which should be used to characterize the constraint level.

For the TSM on the in-plane constraint Q, plane strain condition is usually assumed for the specimen. However, the stress field varied through the thickness of the specimen resulting in different constraint levels, especially for the out-of-plane stress σ_{33}. The out-of-plane constraint parameter T_z is calculated to investigate the thickness effect on the fracture toughness, which is a function of location (r, θ, z) in the polar coordinates at the crack tip. In the case of small strains and a sharp crack tip, T_z = 0.5 for plane strain and T_z = 0 for plane stress. **Figure 8** shows parameter T_z ahead of the crack tip at different thickness locations z for a CT specimen with B = 25 mm. T_z values vary with the distance ahead of the crack tip at a certain thickness location. In order to be consistent with the calculation of Q, value T_z at distance r = 2J/σ_0 from the crack tip is considered.

The three parameters (J integrity, Q, and T_z) change with the crack tip location over the thickness. Generally, an average value along the crack front J_{ave} is considered for the test specimens. In fact, the Q parameter is calculated using the stress field on each layer with different out-of-plane constraints. Therefore, the tested value can be corrected using J and Q on the layer where it is the closest to the average J_{ave}. **Figure 9** shows the corrected fracture toughness to J_{CQ} with Q = 0 from the average values of SENB and CT specimens based on the global approach. The fracture toughness values tested by different specimens are also plotted in the figure with the scatter. In **Figure 9A**, the constraint level at the midplane of the specimen (z = 0) and the average values of J and Q are adopted to scale the fracture toughness. It can be seen that a lower corrected fracture toughness J_{CQ} will be obtained using the average values of J and Q from the same specimen, compared with that using the constraint level at the midplane. For the two crack sizes, the scaled fracture toughness obtained on the

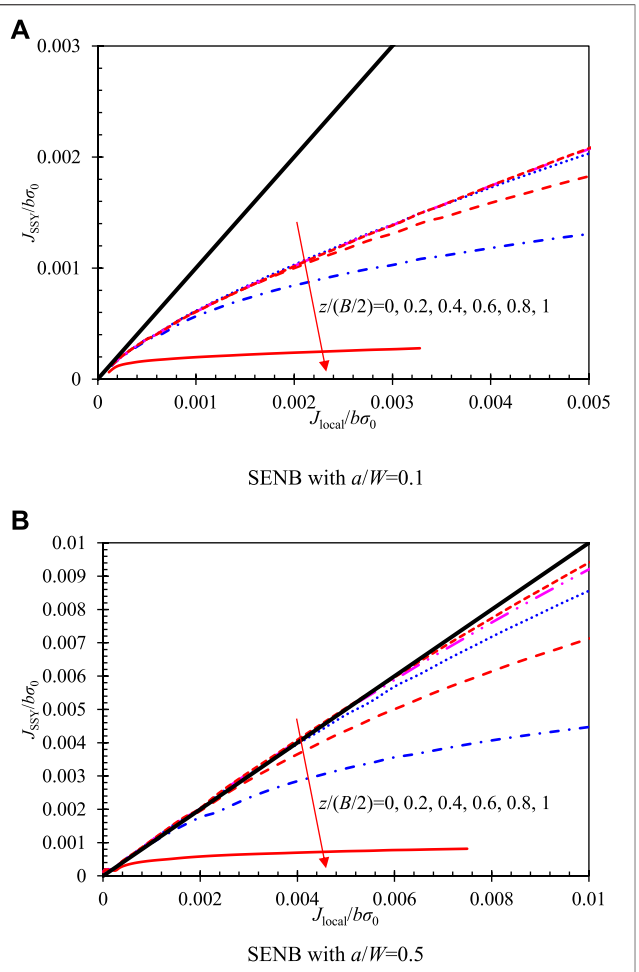

FIGURE 7 | Fracture toughness scaling relationship for SENB specimens on the 2D SSY model. **(A)** SENB with $a/W = 0.1$. **(B)** SENB with $a/W = 0.5$.

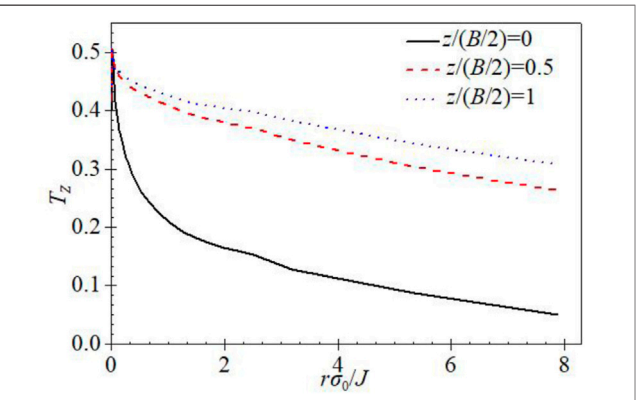

FIGURE 8 | T_z ahead of the crack tip at different thickness location z for a CT specimen with $B = 25$ mm.

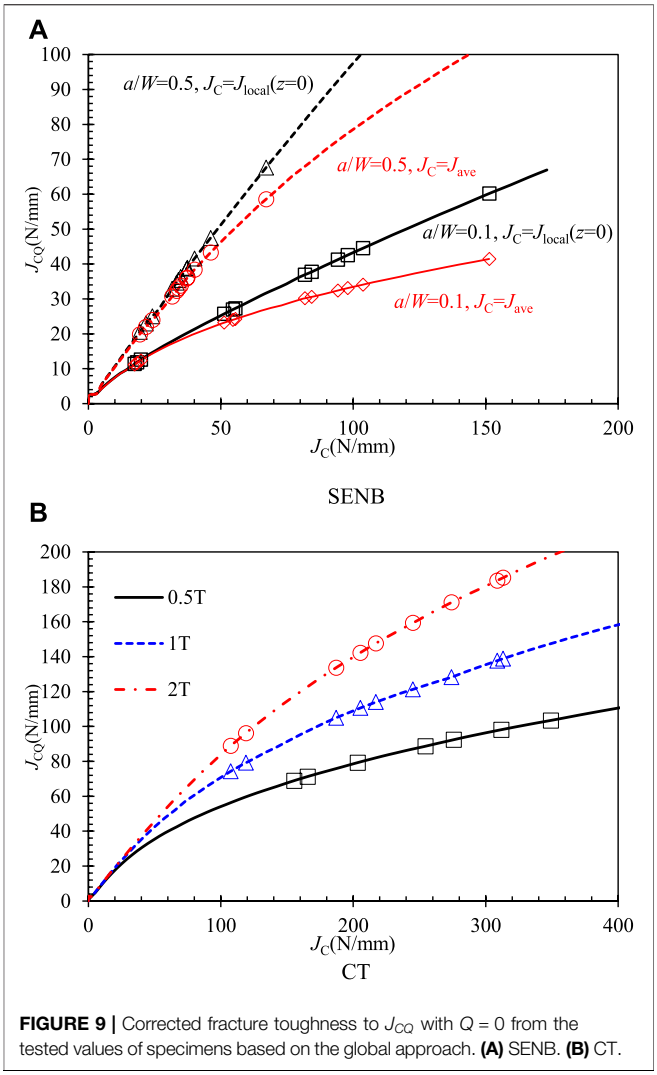

FIGURE 9 | Corrected fracture toughness to J_{CQ} with $Q = 0$ from the tested values of specimens based on the global approach. **(A)** SENB. **(B)** CT.

low constrain with $a/W = 0.1$ may be lower than that with $a/W = 0.5$. Due to the scatter of the tested values, the scaled fracture toughness is also dispersive significantly. This will be discussed in the following section.

For the CT specimens with different thicknesses, the corrected fracture toughness to J_{CQ} is shown in **Figure 9B**, using the average values of J and Q along the thickness. The corrected toughness J_{CQ} under plane strain with $Q = 0$ by the test values of 0.5T specimens is the smallest among the three thickness values, which presents a high level of constraint.

4.3 Scaled Toughness by Weibull Stress

The local approach to fracture has been successfully applied to scale the fracture toughness tested by CT specimens with different thicknesses, SENB specimens with different crack lengths, or different specimen configurations. As the scale

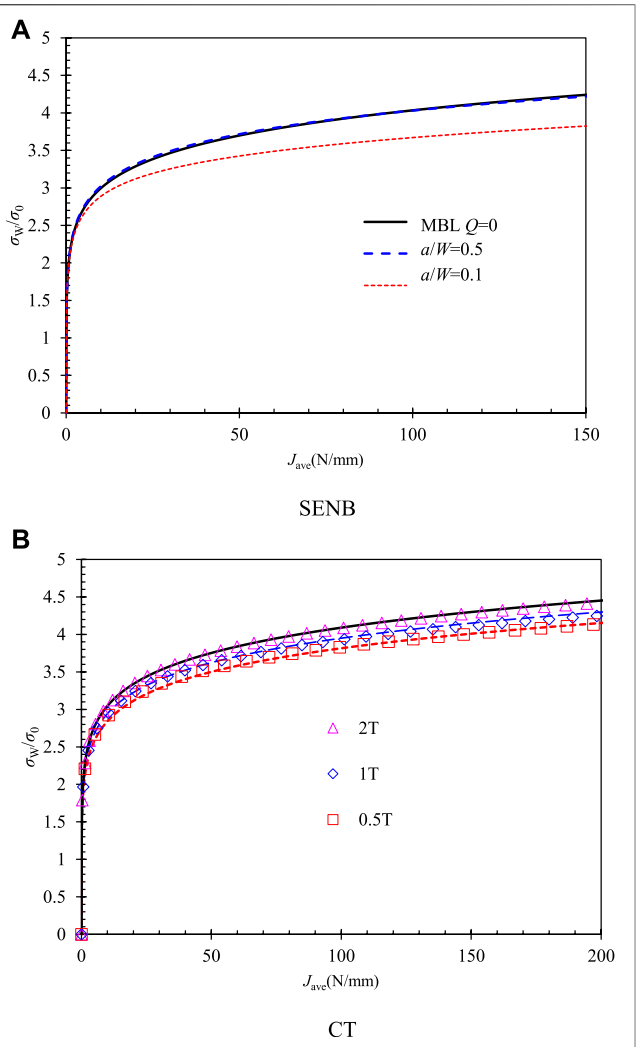

FIGURE 10 | Weibull stress varied with the applied J average for different models. **(A)** SENB. **(B)** CT.

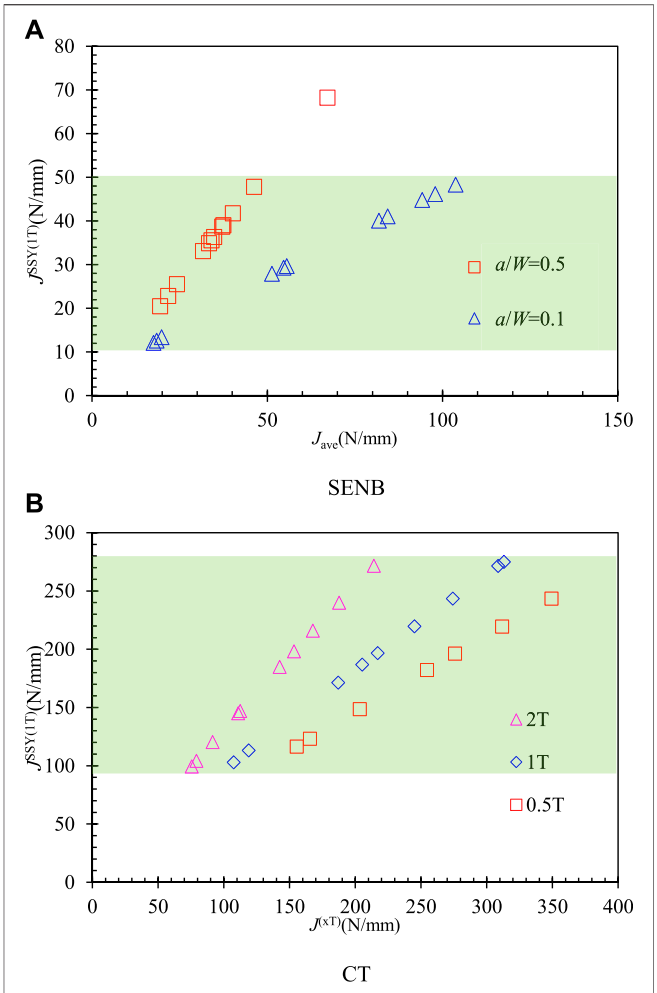

FIGURE 11 | Corrected fracture toughness to J_{SSY} from the average values of SENB and CT specimens on the local approach. **(A)** SENB. **(B)** CT.

parameter in the local approach, Weibull stress should be calculated. A solution of Weibull stress as a function of in-plane constrain Q has been deduced by Li et al.) 2019), but the thickness effect is not available. Therefore, the Weibull stress was calculated according to the stress filed from finite element analysis. The fracture toughness tested by different specimens can be scaled to that under the SSY condition with the same Weibull stress.

Figure 10 shows the Weibull stress for different configurations with the parameter $m = 20$ (Wasiluk et al., 2006). The value of parameter m may affect the absolute value of Weibull stress, which may depend on the specimen configuration and temperature (Qian et al., 2018b). In this work, the original Beremin local approach is adopted. The Weibull stress values calculated by the MBL model with the SSY under plane strain are higher than that by specimen configurations. Because the principal stress in the fracture process zone is considered, the Weibull stress is available to characterize the constraint, including the in-plane and out-of-plane constraints. From **Figure 10A**, it can be seen that the Weibull stress of the SENB specimen with a depth crack a/W = 0.5 is consistent with that of the MBL model with $Q = 0$. For the CT specimens shown in **Figure 10B**, the Weibull stress of the CT specimen is similar to that of the MBL models. It means that the CT specimens have a high constraint level. Meanwhile, a thin specimen presents lower Weibull stress than a thick specimen, which is caused by the loss of constraint.

The assumption with the same Weibull stress, the tested fracture toughness $J^{(xT)}$ of a specimen with the thickness of xT, can be transferred to be the equivalent SSY value of a 1T specimen $J^{SSY(1T)}$. **Figure 11** shows the corrected fracture toughness to J_{SSY} from the average values of SENB and CT specimens with the same Weibull stress. It can be seen that the equivalent SSY value distributes uniformly in the region of 10–50 N/mm for the SENB specimens and 100–270 N/mm for the CT specimens.

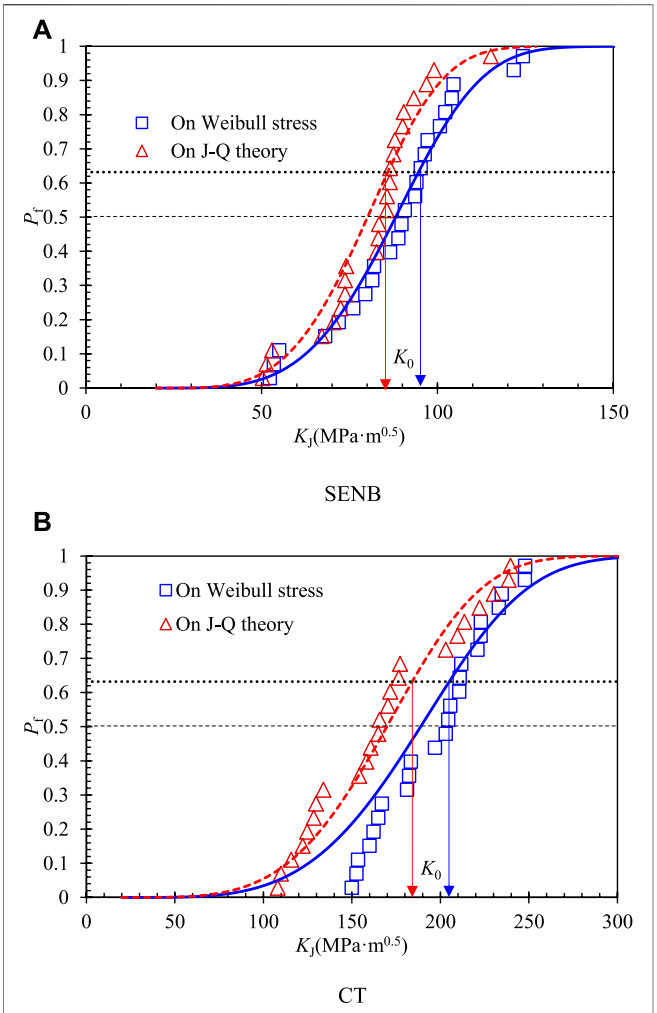

FIGURE 12 | Cumulative failure probability of the scaled toughness on the two approaches. **(A)** SENB. **(B)** CT.

4.4 Comparisons of Scaled Toughness

Using the TSMs by the global approach on the *J-Q* theory and the local approach on the Weibull stress, the scaled values of fracture toughness $J^{SSY(1T)}$ are obtained and comprised. According to **Eq. 8**, the scaled toughness $K_J^{SSY(1T)}$ can be calculated for a configuration with different constraint levels. As the scatter plots in **Figure 12**, the scaled toughness values are plotted with the rank probabilities. The scaled toughness on the Weibull stress will be higher than that on the *J-Q* theory.

Furthermore, a three-parameter Weibull distribution is used to characterize the scatter of the scaled toughness, as shown in **Figure 12** by lines. The cumulative distribution function of the scaled toughness can be described as

$$P_f = 1 - \exp\left(-\left(\frac{K_{JC} - K_{min}}{K_0 - K_{min}} \right)^4 \right), \tag{10}$$

where $K_{min} = 20\text{MPa}\sqrt{\text{m}}$ for common ferritic steels (Wasiluk et al., 2006), and K_0 is a scale parameter of the Weibull distribution. According to the maximum likelihood estimation, K_0 can be estimated using the scaled toughness by

$$K_0 = \left(\sum_{i=1}^{n} \frac{(K_{JC(i)} - K_{min})^4}{r - 0.3068} \right)^{1/4} + 20, \tag{11}$$

where n denotes the number of toughness values in each data set with the number of uncensored tests (six minimum) (Gao et al., 1999). For the CT specimens with a thickness other than 1T, the scaled toughness values should be adjusted to their 1T equivalent values by

$$K_{JC(1T)} = K_{min} + \left(K_{JC}^{xT} - K_{min} \right) \left(\frac{B^{xT}}{B^{1T}} \right), \tag{12}$$

where B^{1T} denotes the 1T specimen size with the thickness of 25 mm and B^{xT} denotes the corresponding thickness of the test specimen.

According to **Eqs 10–12**, we can estimate the scale parameter K_0 using the scaled toughness obtained by the global approach on the *J-Q* theory and the local approach on the Weibull stress. **Figure 12** shows the cumulative failure probability with the estimated scale parameter K_0 as listed in **Table 2**. At the temperature of −100°C near the ductile–brittle transition temperature, there is a slight absolute error between the K_0 values on the *J-Q* theory and Weibull stress compared with that at −40°C. However, the relative error is about 10% at either −100°C or −40°C. This may be caused by the application of the average of J and Q, which gives a lower corrected fracture toughness J_{CQ} than that at the midplane $z = 0$, as discussed in **Section 4.2**. In addition, an m-th power of the principal stress σ_1 near the midplane $z = 0$ brings about a high weight during the calculation of Weibull stress.

TABLE 2 | Estimated scale parameter K_0 by two approaches (MPa$\sqrt{\text{m}}$).

Temperature	−100°C	−40°C
J-Q theory	85.88	184.09
Weibull stress	94.62	205.00

5 CONCLUSION

Some toughness scaling models (TSMs) were proposed to transfer the tested value to fracture toughness under small-scale yielding. Combined with the tested data by SENB specimens with different crack sizes and CT specimens with different thicknesses, the scaled fracture toughness is investigated on the global and local approaches to fracture. Some conclusions can be summarized as follows:

1) The Q parameter depends on the thickness location. A corrected Q value with the average J should be used to characterize the constraint level, combined with the thickness effect.
2) A lower corrected fracture toughness J_{CQ} will be obtained using the average values of J and Q from the same specimen, compared with that using the constraint level at the midplane.

3) Using the single variable of Weibull stress σ_W, the toughness can be scaled, including the effect of in-plane and out-of-plane constraints.
4) The estimated scale parameter K_0 using the scaled toughness obtained by the global approach on the *J-Q* theory is reasonable in agreement with that of the local approach on the Weibull stress with a relative error of about 10%.

DATA AVAILABILITY STATEMENT

The original contributions presented in the study are included in the article/Supplementary Material. Further inquiries can be directed to the corresponding author.

AUTHOR CONTRIBUTIONS

Conceptualization, YuL; methodology, WJ; software, YaL and MZ; validation, WJ and MZ; formal analysis, WJ; investigation, YuL; writing—original draft preparation, WJ and YaL; writing—review and editing, YuL and MZ; funding acquisition, YuL. All authors have read and agreed to the published version of the manuscript.

FUNDING

This research was funded by the National Key R&D Program of China, Grant no. 2020YFB1506100.

REFERENCES

Anderson, T. L., Stienstra, D., and Dodds, R. H. (1994). A Theoretical Framework for Addressing Fracture in the Ductile-Brittle Transition Region. *ASTM Spec. Tech. Publ.* 1207, 186. doi:10.1520/stp13706s

ASTM International (2020). *ASTM E1820-20b, A. Standard Test Method for Measurement of Fracture Toughness*. West Conshohocken, PA: ASTM International. doi:10.1520/E1820-20B

Barbosa, V. S., and Ruggieri, C. (2020). A Simplified Estimation Procedure for the Weibull Stress Parameter, M, and Applications to Predict the Specimen Geometry Dependence of Cleavage Fracture Toughness. *Int. J. Press. Vessels Pip.* 188, 104228. doi:10.1016/j.ijpvp.2020.104228

Dodds, R. H., Anderson, T. L., and Kirk, M. T. (1991). A Framework to Correlate a/W Ratio Effects on Elastic-Plastic Fracture Toughness (JC). *Int. J. Fract.* 48, 1–22. doi:10.1007/bf00012499

EDF Energy Nuclear Generation Ltd (2015). *Assessment of the Integrity of Structures Containing Defects*, R6. Revision 4, with updates to Amendment 11. Gloucester, United Kingdom.

Gao, X., and Dodds Jr, R. H. (2001). An Engineering Approach to Assess Constraint Effects on Cleavage Fracture Toughness. *Eng. Fract. Mech.* 68, 263–283. doi:10.1016/s0013-7944(00)00102-8

Gao, X., and Dodds, R. H. (2000). Constraint Effects on the Ductile-To-Brittle Transition Temperature of Ferritic Steels: a Weibull Stress Model. *Int. J. Fract.* 102, 43–69. doi:10.1023/A:1007526006632

Gao, X., Dodds, R. H., Jr, Tregoning, R. L., Joyce, J. A., and Link, R. E. (1999). A Weibull Stress Model to Predict Cleavage Fracture in Plates Containing Surface Cracks. *Fatigue & Fract. Eng. Mater. Struct.* 22, 481–493. doi:10.1046/j.1460-2695.1999.00202.x

Gao, X., Joyce, J. A., and Roe, C. (2008). An Investigation of the Loading Rate Dependence of the Weibull Stress Parameters. *Eng. Fract. Mech.* 75, 1451–1467. doi:10.1016/j.engfracmech.2007.07.007

Gao, X., Ruggieri, C., and Dodds Jr, R. H. (1998). Calibration of Weibull Stress Parameters Using Fracture Toughness Data. *Int. J. Fract.* 92, 175–200. doi:10.1023/a:1007521530191

Guo, W. L. (1995). Elastoplastic 3-Dimensional Crack Border Field .3. Fracture Parameters. *Eng. Fract. Mech.* 51, 51–71. doi:10.1016/0013-7944(94)00215-4

Heerens, J., and Hellmann, D. (2002). Development of the Euro Fracture Toughness Dataset. *Eng. Fract. Mech.* 69, 421–449. doi:10.1016/s0013-7944(01)00067-4

Horn, A. J., and Sherry, A. H. (2010). Prediction of Cleavage Fracture from Non-sharp Defects Using the Weibull Stress Based Toughness Scaling Model. *Int. J. Press. Vessels Pip.* 87, 670–680. doi:10.1016/j.ijpvp.2010.10.007

Horn, A. J., Cicero, S., and Andres, D. (2020). Out-of-plane Constraint Loss in Three Point Bend Specimens with Notches. *Int. J. Press. Vessels Pip.*, 180, 104025. doi:10.1016/j.ijpvp.2019.104025

International Organization for Standardization (2016). *ISO 12135, Metallic Materials - Unified Method of Test for the Determination of Quasistatic Fracture Toughness*. Vernier, Geneva, Switzerland.

Ishihara, K., Hamada, T., and Meshii, T. (2017). T-scaling Method for Stress Distribution Scaling under Small-Scale Yielding and its Application to the Prediction of Fracture Toughness Temperature Dependence. *Theor. Appl. Fract. Mech.* 90, 182–192. doi:10.1016/j.tafmec.2017.04.008

Li, Y., Wang, Z., Lei, Y., Qian, G., Zhou, M., Gao, Z., et al. (2019). Weibull Stress Analysis in Local Approach to Fracture. *Theor. Appl. Fract. Mech.* 104, 102379. doi:10.1016/j.tafmec.2019.102379

Link, R. E., and Joyce, J. A. (1996). *Application of Fracture Toughness Scaling Models to the Ductile-To-Brittle Transition*. No. NUREG/CR-6279. Washiton DC: Nuclear Regulatory Commission.

Ma, H. S., Wang, G. Z., Liu, S., Tu, S. T., and Xuan, F. Z. (2016). Three-dimensional Analyses of Unified Characterization Parameter of In-Plane and Out-Of-Plane Creep Constraint. *Fatigue Fract. Engng Mater Struct.* 39, 251–263. doi:10.1111/ffe.12361

Meshii, T., and Ishihara, K. (2018). "Application of the T-Scaling Method to Predict Fracture Toughness under Compressive Residual Stress in the Transition Temperature Region," in ASME 2018 Pressure Vessels and Piping Conference, Prague, Czech Republic, July 15–20, 2018.

Mostafavi, M., Smith, D. J., and Pavier, M. J. (2010). Reduction of Measured Toughness Due to Out-Of-Plane Constraint in Ductile Fracture of Aluminium Alloy Specimens. *Fatigue Fract. Eng. M.* 33, 724–739. doi:10.1111/j.1460-2695.2010.01483.x

Mostafavi, M., Smith, D. J., and Pavier, M. J. (2011). A Micromechanical Fracture Criterion Accounting for In-Plane and Out-Of-Plane Constraint. *Comput. Mater. Sci.* 50, 2759–2770. doi:10.1016/j.commatsci.2011.04.023

Neimitz, A., and Dzioba, I. (2015). The Influence of the Out-Of- and In-Plane Constraint on Fracture Toughness of High Strength Steel in the Ductile to Brittle Transition Temperature Range. *Eng. Fract. Mech.* 147, 431–448. doi:10.1016/j.engfracmech.2015.07.017

Neimitz, A., and Galkiewicz, J. (2006). Fracture Toughness of Structural Components: Influence of Constraint. *Int. J. Press. Vessels Pip.* 83, 42–54. doi:10.1016/j.ijpvp.2005.10.001

Neimitz, A., and Lipiec, S. (2021). Fracture Toughness Correction Due to the in- and Out-Of-Plane Constraints. *Theor. Appl. Fract. Mech.* 112, 102844. doi:10.1016/j.tafmec.2020.102844

Neimitz, A., Graba, M., and Gałkiewicz, J. (2007). An Alternative Formulation of the Ritchie-Knott-Rice Local Fracture Criterion. *Eng. Fract. Mech.* 74, 1308–1322. doi:10.1016/j.engfracmech.2006.07.015

Nevalainen, M., and Dodds, R. H. (1996). Numerical Investigation of 3-D Constraint Effects on Brittle Fracture in SE(B) and C(T) Specimens. *Int. J. Fract.* 74, 131–161. doi:10.1007/bf00036262

Nikishkov, G. P., and Matvienko, Y. G. (2016). Elastic-plastic Constraint parameterAfor Test Specimens with Thickness Variation. *Fatigue Fract. Engng Mater Struct.* 39, 939–949. doi:10.1111/ffe.12390

O'dowd, N. P., and Shih, C. F. (1992). Family of Crack-Tip Fields Characterized by a Triaxiality Parameter-2. Fracture Applications. *J. Mech. Phys. Solids* 40, 939–963. doi:10.1016/0022-5096(92)90057-9

O'Dowd, N. P. (1995). Applications of Two Parameter Approaches in Elastic-Plastic Fracture Mechanics. *Eng. Fract. Mech.* 52, 445–465. doi:10.1016/0013-7944(95)00033-r

Pan, J., and Yin, M. (2021). A Study on Fracture Toughness Based on a Modified Beremin Model. *J. Mater. Eng. Perform.* 30, 8309–8321. doi:10.1007/s11665-021-06072-w

Qian, G., Cao, Y., Niffenegger, M., Chao, Y. J., and Wu, W. (2018). Comparison of Constraint Analyses with Global and Local Approaches under Uniaxial and Biaxial Loadings. *Eur. J. Mech. - A/Solids* 69, 135–146. doi:10.1016/j.euromechsol.2017.12.006

Qian, G., Lei, W.-S., Niffenegger, M., and González-Albuixech, V. F. (2018). On the Temperature Independence of Statistical Model Parameters for Cleavage Fracture in Ferritic Steels. *Philos. Mag.* 98, 959–1004. doi:10.1080/14786435.2018.1425011

Ruggieri, C., and Dodds, R. H. (1996). A Transferability Model for Brittle Fracture Including Constraint and Ductile Tearing Effects: a Probabilistic Approach. *Int. J. Fract.* 79, 309–340. doi:10.1007/bf00018594

Ruggieri, C., and Dodds, R. H. (2018). A Local Approach to Cleavage Fracture Modeling: An Overview of Progress and Challenges for Engineering Applications. *Eng. Fract. Mech.* 187, 381–403. doi:10.1016/j.engfracmech.2017.12.021

Ruggieri, C. (2020). A Modified Local Approach Including Plastic Strain Effects to Predict Cleavage Fracture Toughness from Subsize Precracked Charpy Specimens. *Theor. Appl. Fract. Mech.* 105, 102421. doi:10.1016/j.tafmec.2019.102421

She, C., and Guo, W. (2007). The Out-Of-Plane Constraint of Mixed-Mode Cracks in Thin Elastic Plates. *Int. J. Solids Struct.* 44, 3021–3034. doi:10.1016/j.ijsolstr.2006.09.002

Smith, R. J., Horn, A. J., and Sherry, A. H. (2018). Relating Charpy Energy to Fracture Toughness in the Lower Transition Region Using a Weibull Stress Dependent Energy Scaling Model. *Int. J. Press. Vessels Pip.* 166, 72–83. doi:10.1016/j.ijpvp.2018.06.001

Wasiluk, B., Petti, J. P., and Dodds, R. H. (2006). Temperature Dependence of Weibull Stress Parameters: Studies Using the Euro-Material. *Eng. Fract. Mech.* 73, 1046–1069. doi:10.1016/j.engfracmech.2005.11.006

Xu, J. Y., Wang, G. Z., Xuan, F. Z., and Tu, S. T. (2018). Unified Constraint Parameter Based on Crack-Tip Opening Displacement. *Eng. Fract. Mech.* 200, 175–188. doi:10.1016/j.engfracmech.2018.07.021

Yang, J., Wang, G. Z., Xuan, F. Z., and Tu, S. T. (2013). Unified Characterisation of In-Plane and Out-Of-Plane Constraint Based on Crack-Tip Equivalent Plastic Strain. *Fatigue Fract. Eng. M.* 36, 504–514. doi:10.1111/ffe.12019

Zhao, J., and Guo, W. (2012). Three-parameter K-T-Tz Characterization of the Crack-Tip Fields in Compact-Tension-Shear Specimens. *Eng. Fract. Mech.* 92, 72–88. doi:10.1016/j.engfracmech.2012.06.004

Zhen, Y., Chang, Q., Cao, Y., and Niu, R. (2021). A Novel Unified Characterization Parameter of In-Plane and Out-Of-Plane Constraints Based on Critical CTOA. *Fatigue Fract. Eng. Mater Struct.* 44, 1305–1317. doi:10.1111/ffe.13430

Zhou, M., Li, Y., Lei, Y., Zhu, L., and Wang, W. (2021). Weibull Stress Solutions and Applications under Mixed Mode I-II Loading for 2-D Cracks in Elastic and Elastic-Plastic Materials. *Theor. Appl. Fract. Mech.* 113, 102972. doi:10.1016/j.tafmec.2021.102972

Conflict of Interest: The authors declare that the research was conducted in the absence of any commercial or financial relationships that could be construed as a potential conflict of interest.

Publisher's Note: All claims expressed in this article are solely those of the authors and do not necessarily represent those of their affiliated organizations or those of the publisher, the editors, and the reviewers. Any product that may be evaluated in this article, or claim that may be made by its manufacturer, is not guaranteed or endorsed by the publisher.